Dumbbells in suspension: A numerical study on their dynamics and shear viscosity

Johannes Greber[1], Jochen Bammert[1], Philippe Peyla[2], Walter Zimmermann[1]

[1] Theoretische Physik I, Universität Bayreuth, 95440 Bayreuth, Germany
[2] Laboratoire de Physique Interdisciplinaire, UMR 5588, Université Joseph-Fourier, 38402 Saint Martin d'Heres, France

Abstract. The dynamics of elastic dumbbells in linear shear flow is investigated by fluid particle dynamics simulations at small Reynolds numbers. The positive contribution of a single dumbbell to the effective shear viscosity is determined via the extra stress exerted at the boundaries of the shear cell and the difference to the contributions obtained via the Kramers-Kirkwood formula are described. For a small Weissenberg number and when the mean dumbbell length becomes larger than the mean next-neighbor distance, the contribution of interacting dumbbells to the mean shear viscosity exceeds significantly the contribution of unconnected beads occupying the same volume fraction.

1 Introduction

Particles in a fluid change the viscosity and cause a variety of interesting as well as astonishing flow phenomena [1–3]. The shear viscosity of a suspension increases in the diluted regime linearly with the particle concentration [4, 5] and quadratic effects come into play with the importance of particle-particle interactions [6,7]. Soft particles, such as polymers, may change with their extra dynamical degrees of freedom the macroscopic flow properties of a fluid significantly, especially when the product of the particle relaxation-time and the local shear rate, the so called Weissenberg number, reaches values of the order one. In this regime, but still at small values of the particle Reynolds number, polymers may exhibit a rich dynamics and may give rise to phenomena such as shear thinning [1,2], tumbling [8–13], elastic turbulence [3] or polymer induced, efficient fluid mixing [14]. Vesicles in linear shear flows are deformed as well, leading to various kinds of nonlinear transitions between dynamical states [15,16], a topic reviewed recently in Refs. [17,18].

Flows of suspensions of polymers or vesicles are often modeled by using appropriate constitutive equations for the stress tensor $\underline{\sigma}$ in generalized Navier-Stokes equations [2]. Such models are quite common in the range of small values of the Weissenberg number, corresponding to small particle deformations, and in the regime of small particle concentrations, where particle-particle interactions are still weak. The interactions among many deformable particles in flow may be intricate, especially the nonlinear, long-range hydrodynamic interaction as well as effects of walls

may induce a complex dynamics. Which degrees of freedom are relevant in macroscopic modeling? For this purpose investigations of the dynamics of bead-spring models in flow by computer simulations [27–33] are a powerful tool. Appropriate simulations enable an estimate, for instance, of the relative importance of the dynamics of single soft particles in flow and the particle-particle interactions [27–33]. Well known computational schemes are Brownian dynamics simulations [19,20], multi-particle-collision dynamics [21,22] or lattice Boltzmann methods [23].

Here we investigate the dynamics of a suspension of elastic dumbbells by three dimensional simulations and calculate their contribution to the shear viscosity of the suspension. For this purpose we use fluid particle dynamics (FPD), which was developed by Tanaka and Araki [34] and which is summarized in Sect. 2. It is based on a continuum description of suspended particles in an incompressible fluid, where the viscosity of the solvent is enhanced at the positions of the particles. This approach has been applied successfully to explorations of the dynamics of colloidal particles in complex fluids [35], the polymer coil-globule transition [36], the effect of confinement on the rheology of a suspension of spheres [37], and the effective viscosity of micro-swimmer suspensions [38].

The tumbling dynamics of a single dumbbell in the shear plane and the contribution of a dumbbell to the effective shear viscosity is determined in a direct manner via the applied shear stress at the walls of a shear cell in Sect. 3. The difference between these direct contributions to the shear stress and the dumbbell contribution via the Kramers-Kirkwood approach for deformable dumbbells [2,

39,40] are also described. The effects of many interacting dumbbells in a shear flow is investigated in Sect. 4, where we present a significant enhancement of the effective viscosity in the case of an increasing importance of the dumbbell-dumbbell correlation.

2 Fluid Particle Dynamics and effective viscosity

In fluid particle dynamics simulations a suspension is described by an incompressible single component fluid with a spatially varying viscosity [34],

$$\eta(\mathbf{r}) = \eta_s + \frac{\eta_p - \eta_s}{2} \sum_{i=1}^{N} \left[1 + \tanh \left(\frac{\nu - |\mathbf{r} - \mathbf{r}_i|}{\xi} \right) \right] , \quad (1)$$

where the viscosity is considerably enhanced at the particle positions $\mathbf{r}_i$ ($i = 1, \ldots, N$) to about $\eta_p = 100\eta_s$. The parameter ν describes the range of the local viscosity enhancement around $\mathbf{r}_i$ and ξ the width of the transition regime between the two viscosity levels η_s and η_p. Throughout of this work we choose $\nu = 2$ and $\xi = 0.5$, which corresponds to an effective particle radius $a = 3$.

The dynamics of the velocity field $\mathbf{u}(\mathbf{r}, t)$ of an incompressible fluid of density $\rho = const.$ ($\nabla \cdot \mathbf{u} = 0$) is described by the time-dependent equation

$$\rho \left[\partial_t \mathbf{u} + (\mathbf{u} \cdot \nabla) \mathbf{u} \right] = \nabla \cdot \underline{\underline{\sigma}} , \quad (2)$$

where the stress tensor

$$\underline{\underline{\sigma}} = -p\underline{\underline{I}} + \eta \left(\nabla \mathbf{u} + (\nabla \mathbf{u})^T \right) . \quad (3)$$

includes the spatially varying viscosity field $\eta(\mathbf{r})$ and the pressure field $p(\mathbf{r})$ with the unity matrix $\underline{\underline{I}}$. Eq. (2) is solved on a three dimensional grid (Marker and Cells) with a mesh of length one, by using a projection method [41]. The resulting velocity field, averaged over the range of the enhanced viscosity, is used to update the particle's position, as described in more detail in Refs. [34, 25].

The two beads of a dumbbell are connected by a linear spring with an equilibrium length R_0 of the connection vector $\mathbf{R} = \mathbf{r}_2 - \mathbf{r}_1$, cf. Fig. 1, and the spring constant k. The resulting spring force

$$\mathbf{F}(\mathbf{R}) = f(R)\frac{\mathbf{R}}{R} \quad (4)$$

is proportional the elongation $R(t) - R_0$ with $f(R(t)) = k[R(t) - R_0]$ and acts along the connection vector $\mathbf{R}(\mathbf{t})$. For the sake of simplicity we use harmonic springs, but for FENE springs, as described in Ref. [28], qualitatively similar results are obtained. $\theta \in [0, \pi]$ is the angle enclosed by $\mathbf{R}$ and the undistorted flow direction $\hat{\mathbf{z}}$. In order to exclude overlap between dumbbell beads, we use a short-range repulsive potential $\phi_{LJ} = \alpha/r^{12} - \beta/r^6$ for each bead with a cut-off length of $2a$.

The dumbbells are confined in a rectangular flow channel of size $H_x \times H_y \times H_z$ with $H_x = H_y = 60$ and $H_z = 100$,
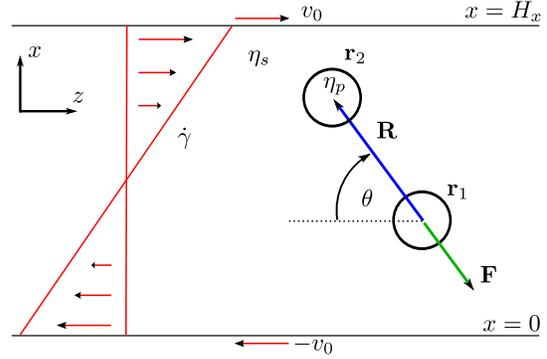

Fig. 1. In FPD suspended particles are modeled by an enhanced viscosity $\eta_p = 100\eta_s$ around their centers at $\mathbf{r}_i$. A dumbbell consists of two beads connected by a spring along the connection vector $\mathbf{R} = \mathbf{r}_2 - \mathbf{r}_1$. Moving the upper and lower plate of the flow channel with constant velocity v_0, we create a linear shear flow with shear rate $\dot{\gamma} = 2v_0/H_x$.

if not stated otherwise. We impose no-slip boundary conditions at the walls in x and y direction and periodic boundary conditions along the z direction. By moving the upper plate at $x = H_x$ with a velocity $v_0\hat{\mathbf{z}}$ and the lower plate at $x = 0$ with $-v_0\hat{\mathbf{z}}$, as indicated in Fig. 1, we create a linear shear flow of shear rate

$$\dot{\gamma} = \frac{2v_0}{H_x} . \quad (5)$$

For a dumbbell a typical time scale τ may be introduced in terms of the Stokes friction $\zeta = 6\pi\eta_s a$ as well as the dimensionless Weissenberg number W:

$$\tau = \frac{\zeta}{k} \quad \text{and} \quad \text{W} = \dot{\gamma}\tau . \quad (6)$$

The effective viscosity of a suspension at constant shear stress is determined in our system by the xz component of the stress tensor $\underline{\underline{\sigma}}$ averaged over the whole surface of the moving boundaries:

$$\eta_{eff}(t) = \frac{\bar{\sigma}_{xz}(x = H_x) + \bar{\sigma}_{xz}(x = 0)}{2\dot{\gamma}} . \quad (7)$$

According to the tumbling motion of dumbbells $\eta_{eff}(t)$ is a function of time and its time average is denoted by

$$\bar{\eta}_{eff} = \langle \eta_{eff}(t) \rangle . \quad (8)$$

The effective averaged viscosity of a homogeneous suspension of independent spheres can be represented in terms of a virial expansion with respect to the volume fraction Φ occupied by the particles in suspension:

$$\bar{\eta}_{eff}(\Phi) = \eta_s \left(1 + w_1\Phi + w_2\Phi^2 + \mathcal{O}\left(\Phi^3\right) \right) . \quad (9)$$

In the dilute regime, where hydrodynamic particle-particle interactions become negligible, Einstein determined the first coefficient: $w_1 = 2.5$ [4,5]. The second order coefficient $w_2 = 5.2$ was determined by Batchelor and Green

[6], which has later been evaluated including the high frequency regime as well by Felderhof and Cichocki to $w_2 = 5.0$ [7]. In FPD simulations it was shown that both coefficients w_1 and w_2 are changed in the case of strong confinement of a suspension of spheres [38]. How the shape of suspended objects influences the viscosity have been also investigated [42].

Two useful quantities for a characterization of the dumbbell dynamics and the shear viscosity are the relative deformation

$$\varepsilon(t) = \frac{R(t) - R_0}{R_0}, \tag{10}$$

and the spatially averaged relative viscosity change induced by the dumbbells,

$$\Delta\eta(t) = \frac{\eta_{eff}(t) - \eta_s}{\eta_s}. \tag{11}$$

In simulations of colloidal suspensions the contributions of particles to the shear viscosity are often determined indirectly via the Kramers-Kirkwood formula of the stress tensor [2,39],

$$\underline{\underline{\lambda}} = -\langle \mathbf{R}(t) \otimes \mathbf{F}(t) \rangle, \tag{12}$$

whereby this formula is derived under the assumption of point like beads at the ends of dumbbells, i. e. with the bead radii much smaller than the bead distance, $a \ll R_0$. The time dependence of the connection vectors $\mathbf{R}_i(t)$ of dumbbells and the spring forces $\mathbf{F}_i(t)$ in this formula may be obtained from numerical simulations of the dumbbell dynamics.

In this work we evaluate the formula (12) only for a single dumbbell in order to estimate the differences between the dumbbell contribution to the viscosity, when the dumbbell is composed of point like beads, and a direct determination of the dumbbell contribution to the shear viscosity change in Eq. (11). For this purpose we take the time dependence of $\mathbf{R}(t)$ obtained from simulations and calculate the time dependence of $\underline{\underline{\lambda}}(t)$ and compare it with Eq. (11).

3 Dynamics of a single dumbbell

In this section, the rotation of a dumbbell in the shear plane is investigated, where its contribution to the relative shear viscosity change $\Delta\eta(t)$ takes its largest values. This is compared with the contribution of two independent beads to $\Delta\eta(t)$ as well as with the time dependence of the dumbbell contribution to the stress tensor, as calculated in terms of the dumbbell conformation via the Kramers-Kirkwood formula given by Eq. (12).

With increasing values of the Weissenberg number, W, the duration of a dumbbell rotation in the shear plane decreases and the temporal dumbbell deformation increases. The compression (stretch) of a dumbbell spring increases during the first (second) quarter of a dumbbell turn, as indicated in Fig. 2 by the relative extension $\varepsilon(\theta)$ for W = 0.2
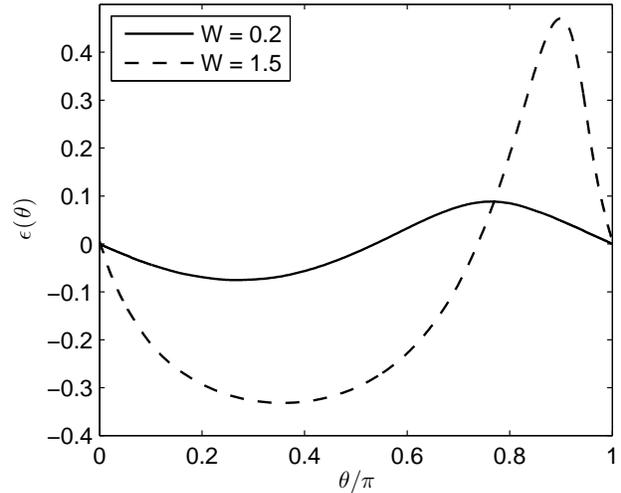

Fig. 2. The relative dumbbell deformation $\varepsilon(\theta)$ [cf. Eq. (10)] is shown during one half turn in the shear plane for $R_0 = 10$ and two different values of the Weissenberg number: W = 0.2 and W = 1.5.
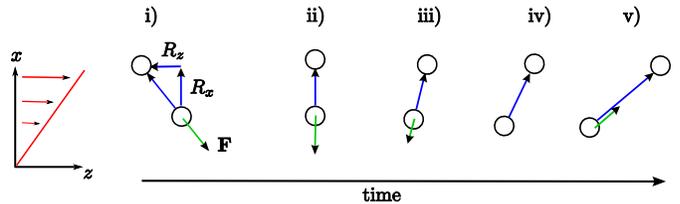

Fig. 3. The sketch of the tumbling motion at a high Weissenberg number illustrates the connection between dumbbell dynamics and $\lambda_{xz}(t)$.

and W = 1.5. In the range of W $\ll$ 1 the dumbbell deformation adapts nearly instantaneously to the balance between the spring and friction force. Accordingly, the dumbbell deformation $\varepsilon(\theta)$ vanishes at about $\theta \sim \pi/2$, where for a short moment during a dumbbell turn either compressing or extending - frictional forces become rather small.

This is different in the range of larger values of W, where dumbbell turns are faster with respect to the relaxation time. In this range the dumbbell relaxation follows with a finite delay the temporal difference between the spring and the friction forces acting on the dumbbell beads. For the Weissenberg number W = 1.5 a dumbbell is strongly compressed by viscous friction forces during the first quarter of a turn, which is followed by a rather quick dumbbell rotation on the scale of the scale of the relaxation time, so that the dumbbell spring is still not relaxed when the dumbbell orientation passes the angle $\theta = \pi/2$. In this case the relative dumbbell deformation $\varepsilon(\theta)$ becomes zero at a delayed angle $\theta_0 > \pi/2$. The phase shift $\theta_0 - \pi/2 > 0$ increases with the Weissenberg number W and causes an asymmetric θ dependence of $\varepsilon(\theta)$ with respect to $\pi/2 < \theta_0 < \pi$, as shown in Fig. 2.
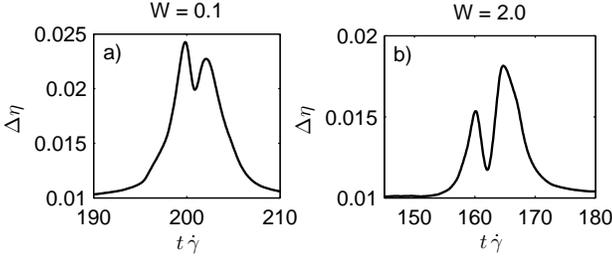
Fig. 4. Part a) and b) show the time dependence of the relative viscosity chance $\Delta\eta(t)$ during one half turn of a dumbbell at two different values of the Weissenberg number: W = 0.1 (left) and W = 2.0 (right).
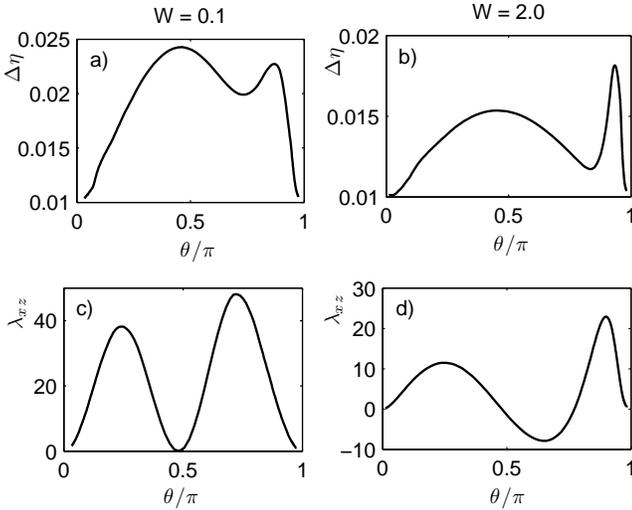

Fig. 5. Part a) and b) show the relative viscosity chance $\Delta\eta(\theta)$ during one half turn of a dumbbell at two different values of the Weissenberg number: W = 0.1 (left) and W = 2.0 (right). Parts c) and d) show $\lambda_{xy}(\theta)$ for the same parameters.

A complementary view on the angle dependence of the relative deformation $\varepsilon(\theta)$ provides Fig. 3. This figure shows the connection vector **R** (blue) at different values of the dumbbell orientation angle θ as well as the spring force **F** (green) acting on one bead, whereby $-$**F** acts on the opposite bead. The figure indicates that the force **F**, being either parallel or anti-parallel to **R**, vanishes and changes its sign at the angle $\theta_0 > \pi/2$, where the relative extension $\varepsilon(\theta)$ passes zero in Fig. 2.

The contribution of a dumbbell to the relative shear-viscosity change $\Delta\eta(t)$ varies as a function of time and the orientational angle θ as illustrated by numerical data in Fig. 4 and in the upper part of Fig. 5 for two different values of W.

The contribution of deformable particles in a fluid to the shear viscosity is often calculated via the stress tensor λ_{ij} [2], which may be calculated in terms of deformation data obtained from simulations. For a dumbbell the ma-
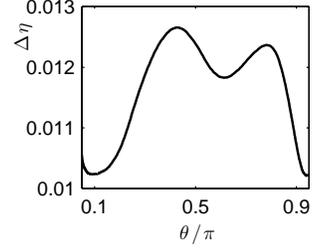

Fig. 6. The contribution of two unconnected beads to the relative viscosity chance $\Delta\eta(t)$ in a shear cell as a function of the angle θ, enclosed by the connection vector between two beads and the streamlines.

trix element $\lambda_{xz}(t)$ in Eq. (12) takes the following form:

$$\lambda_{xz}(t) = -f(R)\frac{R}{2}\sin(2\theta). \qquad (13)$$

It depends on the dumbbell extension $R(t) - R_0$ via $f(R)$ and on the orientational angle θ. For small values of W the two functions $\sin(2\theta)$ and $R(t) - R_0$ pass zero near the perpendicular dumbbell orientation, i. e. for $\theta \sim \pi/2$, and therefore $\lambda_{xz}(\theta \sim \pi/2)$ vanishes as in Fig. 5c). For larger values of W the function $R(\theta) - R_0$ passes zero at an angle θ_0 larger than $\pi/2$, cf. Fig. 2, and $\lambda_{xz}(\theta)$ becomes negative between both zeros, as can be seen in Fig. 5d). On the other hand the directly determined relative viscosity change $\Delta\eta$ is always positive in Fig. 5a) and Fig. 5b) - as expected. The fact, that λ_{xz} becomes negative in an intermediate range, shows the limitations of the Kramers-Kirkwood-formula for a determination of the contribution of deformable particles to the stress tensor of a suspension and therefore to the shear viscosity of a suspension of dumbbells or other deformable particles.

In Fig. 4a) and Fig. 4b) the dumbbell axis is nearly parallel to the flow lines for small and large values of $\dot\gamma t$. In this range the dumbbell contribution to $\Delta\eta$ is similar to the contribution of two unconnected beads with its connection vector parallel to the flow lines, as indicated in Fig. 6. In both cases the relative shear viscosity change is about $\Delta\eta \simeq 0.01$ and therefore the contribution to $\Delta\eta$ of a dumbbell with the connection vector parallel to the flow lines is essentially caused by the rotating beads of finite diameter at both ends of a dumbbell.

The dependence of $\Delta\eta(\theta)$ on the angle θ of the connection vector between two unconnected beads in Fig. 6 shows two maxima, similar as for a dumbbell in Fig. 5a) and Fig. 5b). The hydrodynamic interaction between the two rotating beads is in both cases comparable at similar bead distances. This interaction causes the major contribution to $\Delta\eta(\theta)$ in Fig. 6 for two unconnected beads, whereas in the case of dumbbells the spring force causes modifications, leading to the differences between the results shown in Fig. 6 at the one hand and on the other hand in Fig. 5a) and Fig. 5b).

In our numerical examples, the maxima of $\Delta\eta$ are in the range of small values of W for dumbbells roughly by a

factor of two larger as for unconnected beads - due to the spring force. This enhancement becomes larger by decreasing the ratio between the bead diameter and the dumbbell length. It becomes smaller by increasing the Weissenberg number W. Note, that W may be enhanced by increasing the shear rate or by decreasing the spring constant, i. e. large values of W are closer to the case of unconnected beads.

The reason for a higher contribution of a dumbbell to $\Delta\eta$ is as follows. During a dumbbell turn the dumbbell spring is most of the time either compressed or stretched and the forces involved during a dumbbell compression or stretch are actually exerted by the moving boundaries of the shear cell via the viscous fluid, which causes an enhanced contribution to $\Delta\eta(t)$. Between the ranges where the dumbbell is compressed or stretched, the dumbbell passes rather quickly to a vertical orientation, as indicated by Fig. 4a) and Fig. 4b). In this range the spring becomes relaxed and leads to a reduction of $\Delta\eta$ in an intermediate state.

4 Viscosity of a dumbbell suspension

In a suspension of dumbbells, excluded volume and the nonlinear hydrodynamic interactions lead to a far more complex dynamics of dumbbells than in the case of one isolated dumbbell, as discussed in the previous Sect. 3. This is demonstrated by simulations of 80 dumbbells in a box filled with a Newtonian fluid, where the dumbbells are initially placed on a lattice with the same orientation angle θ. After a transient regime of redistribution of
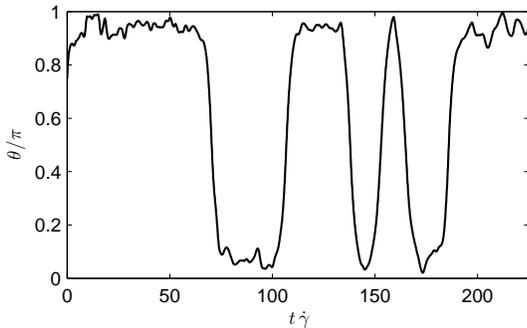

Fig. 7. The temporal behavior of the orientation angle $\theta(t)$ of an individual dumbbell in a suspension of 80 objects (corresponding to $\Phi = 0.05$) behaves rather irregular. The dumbbell extension was $R_0/a = 3.33$ and $W = 2.0$.

dumbbells in shear flow a typical temporal behavior of the angle $\theta(t)$ of a single dumbbell out of 80 is shown in Fig. 7. It confirms that dumbbells are most of their time with $\theta \sim 0, \pi$ nearly parallel oriented to the undisturbed flow lines parallel to $\hat{z}$ and the major part of a dumbbell turn takes place during a short period of time. Compared to the dynamics of a single dumbbell in a fluid such turns of dumbbells in suspension take place rather irregularly in time.

The stationary orientational distribution of dumbbells and the effect of the dumbbell dynamics on the time averaged relative viscosity change,

$$\Delta\bar{\eta} = \langle \Delta\eta(t) \rangle, \qquad (14)$$

are both measures of the overall mean response of a suspension to the applied steady shear flow. The distribution function of the bead positions, the deformations of springs and the distribution of the dumbbell orientational angle θ reach in simulations after a transient regime a stationary state, independent of the initial condition. Fig. 8 shows the stationary distribution of the dumbbell orientation-angle $\mathcal{P}(\theta)$, which has maxima around 0 and π, because the dumbbell axis between the subsequent half-rotations stays most of the time close to $\hat{z}$, cf. Fig. 7.

The asymmetry of $\mathcal{P}(\theta)$ and the asymmetry of $\varepsilon(\theta)$ in Fig. 2 with respect to $\theta = \pi/2$ are related to each other and have its origin in the hydrodynamic dumbbell-dumbbell interaction during the shear induced rotations of the beads of the dumbbells and the contribution of the extensional part of the shear flow. The hydrodynamic interaction due to bead rotations is enhanced during the compressed phase of the dumbbell and therefore the dumbbell rotation is quicker in the range $\theta < \pi/2$, leading to a smaller probability of the dumbbell orientation in this range than in $\theta > \pi/2$. This observation is also supported by the θ-dependence of $\Delta\eta$ in Fig. 5.
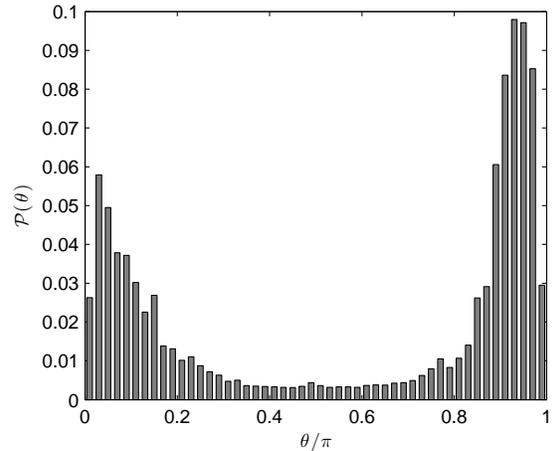

Fig. 8. The time averaged distribution, $\mathcal{P}(\theta)$, of the orientation angle θ as obtained for a suspension of 80 dumbbells in shear flow and Weissenberg number W = 0.21.

According to Eq. (9) one expects for a diluted suspension of independent spheres a linear relation between $\Delta\bar{\eta}$ and the volume fraction Φ. We tested this in simulations by varying the number of beads in the shear cell from 10 up to 320, which corresponds to a variation of the bead-volume fraction between $\Phi = 0.0066$ and $\Phi = 0.1056$. The simulation data obtained for the averaged relative viscosity change $\Delta\bar{\eta}$ are given in Fig. 9 (circles) and it can be seen that for independent beads a linear relation $\Delta\bar{\eta} \propto \Phi$ holds up to about $\Phi^* \simeq 0.015$. Beyond Φ^* the effects of hy-
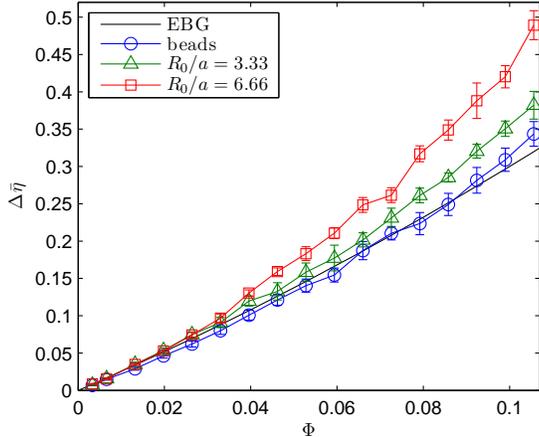
Fig. 9. The averaged relative viscosity $\Delta\bar{\eta} = \langle\Delta\eta\rangle$ is shown for W = 0.33 as a function of the volume fraction Φ for a suspension of spheres (circles) or dumbbells with $R_0/a = 3.33$ (triangles) or $R_0/a = 6.66$ (squares). The solid line is according to the analytical result of Einstein, Batchelor and Green as given by Eq. (9), which deviates from our numerical results beyond $\Phi \simeq 0.08$.

drodynamic particle-particle interaction becomes increasingly stronger and this effect is described in Eq. (9) by the contribution quadratic in Φ. The simulation data for a suspension of independent spheres in Fig. 9 (circles) are approximated by the solid line due to Eq. (9) reasonably well up to a volume fraction $\Phi \approx 0.08$.

The mean distance l between the centers of two spheres decreases with the volume fraction Φ as follows,

$$l = a \left(\frac{4\pi}{3\Phi}\right)^{1/3}. \tag{15}$$

At the volume fraction Φ^* one obtains a mean distance $l^* \approx 6.5a$ and for $l < l^*$ the hydrodynamic particle-particle interaction becomes significant. In the case of dumbbells this length scale has to be compared with the dumbbell extension R_0.

The contribution of a single dumbbell to $\Delta\eta$ deviates from the contribution of two independent beads only significantly during the short temporal range of a dumbbell turn in the range $\theta \sim \pi/2$, as indicated in Fig. 5 and Fig. 6. Therefore, the temporally averaged dumbbell contribution to $\Delta\bar{\eta}$ is nearly equal to the contribution of two independent beads. However, this deviation increases for a fixed number of dumbbells with the dumbbell extension R_0.

If one increases the volume fraction Φ of dumbbells, their extension R_0 or both simultaneously, their contribution to $\Delta\bar{\eta}$ deviates from the contribution of the same number of independent beads because of the following trends. An increasing number of dumbbells increases the dumbbell turns per unit time and therefore their dumbbell contribution to $\Delta\bar{\eta}$. In a dumbbell suspension the motion of pairs of beads is strongly correlated. This leads to an effective extension of the hydrodynamic and excluded volume bead-bead interaction length and simultaneously to

a stronger enhancement of $\Delta\bar{\eta}$ for dumbbells with Φ than for independent beads. These effects together cause the increasing deviations between the data shown in Fig. 9 for independent beads (circles) and for dumbbells of length $R_0 = 3.33a$ (triangles).

For longer dumbbells with $R_0 = 6.66a$ the hydrodynamic and excluded volume interaction is even more enhanced. In addition the length l becomes already for volume fractions $\Phi > 0.015$ smaller than R_0 and the ranges motion of individual dumbbells start of overlap more and more with increasing values of Φ. Both trends cause for dumbbells of length $R_0 = 6.66a$ an even larger contribution to $\Delta\bar{\eta}$ as for same density of dumbbells of length $R_0 = 3.33a$, as can be seen by comparing in Fig. 9 the data obtained for dumbbells of length $R_0 = 6.66a$ (squares) with those obtained for dumbbells of length $R_0 = 3.33a$ (triangles).

How the dumbbell contribution to $\Delta\bar{\eta}$ increases as a function of the relative extension R_0/a for a fixed dumbbell density $\Phi = 0.1056$, is shown in Fig. 10. In this example the effect of dumbbell-dumbbell interaction may enhance the shear viscosity in the range $R_0/a > 6$ by more than 40 percent compared to the same volume fraction of independent beads.
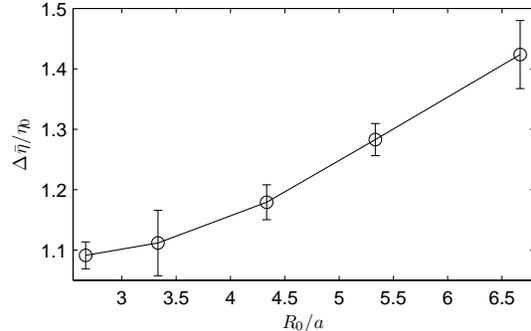

Fig. 10. The relative viscosity $\Delta\bar{\eta}$ as a function of the relative length R_0/a of the undistorted springs of the dumbbells in suspension which occupy the volume fraction $\Phi = 0.1056$ at W = 0.33. η_0 is the viscosity of a suspension of spheres at the same volume fraction.

5 Conclusion

The dynamics of dumbbells in a linear shear flow was investigated by fluid particle dynamics simulations. The numerical results on the tumbling motion of a single dumbbell illustrate, that the effective viscosity in a shear cell is enhanced only during a short part of a dumbbell turn, compared to the case of two independent beads in the fluid. This enhancement of the shear viscosity during a dumbbell turn, however, decreases with increasing values of the Weissenberg number, as one can recognize by com-

paring the results shown in Fig. 4 (a) and in Fig. 4(b). This trend is similar as shear thinning in polymer solutions.

The dumbbell contribution to the shear stress determined via the Kramers-Kirkwood formula becomes negative with larger values of the Weissenberg number for an increasing part of a dumbbells turn. This negative contribution increases with the ratio between the bead diameters and the dumbbell length. The dumbbell dynamics obtained in simultions is often used to determine the dumbbell contribution to the shear stress tensor via Kramers-Kirkwood formula. To the best of our knowledge, there was no comparison between a direction determination of the shear stress contribution of dumbbells and calculations via the Kramers-Kirk-wood formula. It illustrates the limitation of the often used Kramers-Kirk-wood formula for a determination of the dumbbell contribution to the shear viscosity of a suspension because we find in direct simulations at any stage of a dumbbell turn a positive contribution to the shear stress.

Up to a volume fraction $\Phi \simeq 0.08$ of independent spheres in a fluid, we found good agreement between the fluid particle simulations and the Batchelor-Green formula [6] for the effective viscosity of a suspension of unconnected spheres. In the diluted regime dumbbells cause only a slight enhancement of the time-averaged shear viscosity due to the following reasons. Since dumbbells are most of the time nearly parallel oriented to the undisturbed stream lines they contribute to the time-averaged shear viscosity only slightly more than unconnected beads. In addition, in the diluted regime also the hydrodynamic and excluded volume dumbbell-dumbbell interaction is still small.

By increasing the volume fraction of dumbbells in a fluid the hydrodynamic and excluded volume interaction become increasingly more important than for unconnected beads: In a dumbbell suspension a pair of beads performs a correlated motion and therefore, the effective hydrodynamic and excluded volume interaction length is enhanced compared to a suspension of independent beads. This leads in the case of a dumbbell suspension to a significantly stronger contribution to the shear viscosity than for unconnected beads. This effect is especially enhanced when the dumbbell extension exceeds the mean distance between the beads of dumbbells.

Due to dumbbell-dumbbell interactions, the dynamics of a single dumbbell out of a suspension is by far more complex than that of an isolated one in shear flow, similar as the complex polymer dynamics in elastic turbulence. The statistics of the complex dynamics of a suspension of dumbbells and trimers, the possibility of shear thinning effects occurring for both types of bead-spring models in suspension as well as the possibility of turbulent behavior in such suspensions is discussed elsewhere.

References

1. R. G. Larson, *The Structure and Rheology of Complex Fluids* (Oxford University Press, New York, Oxford, 1999).
2. R. B. Bird, C. F. Curtiss, R. C. Armstrong, and O. Hassager, *Dynamics of Polymeric Liquids I, II* (Wiley & Sons, New York, 1987).
3. A. Groisman and V. Steinberg, Nature **405**, 53 (2000).
4. A. Einstein, Ann. Phys. **19**, 289 (1906).
5. A. Einstein, Ann. Phys. **34**, 591 (1911).
6. G. K. Batchelor, J. T. Green, J. Fluid Mech. **56**, 401 (1972).
7. B. Cichocki, B. U. Felderhof, J. Chem. Phys. **89**, 1049 (1988).
8. D. E. Smith and H. P. Babcock and S. Chu, Science **283**, 1724 (1999).
9. R. E. Teixeira, C. M. Schroeder, E. S. G. Shaqfeh, and S. Chu, Macromolecules, **38**, 581 (2005).
10. C. M. Schroeder and R. E. Teixeira and E. S. G. Shaqfeh and S. Chu, Macromolecules, **38**, 1967 (2005).
11. S. Gerashchenko and V. Steinberg, Phys. Rev. Lett. **96**, 038304 (2006).
12. M. Chertkov, I. Kolokolov, V. Lebedev, and K. Turitsyn, J. Fluid Mech. **531**, 251 (2005).
13. C.-C. Huang, G. Stutmann, G. Gompper, R. G. Winkler, EPL **93**, 54004 (2011).
14. A. Groisman and V. Steinberg, Nature **410**, 905 (2001).
15. C. Misbah, Phys. Rev. Lett. **96**, 028104 (2006).
16. V. Kantsler and V. Steinberg, Phys. Rev. Lett. **96**, 036001 (2006).
17. P. M. Vlahovska, T. Podgorski and C. Misbah, Comptes Rendue Physique **10**, 775 (2009).
18. N. J. Zabusky, E. Segre, J. Deschamps, V. Kantsler and V. Steinberg, Phys. Fluids **23**, 041905 (2011).
19. R. M. Jendrejack *et al.*, Phys. Rev. Lett. **91**, 038102 (2003).
20. R. Prabhakar and J. R. Prakash, J. Non-Newtonian Fluid Mech. **116**, 163 (2004).
21. A. Malevanets and R. Kapral, J. Chem. Phys. **112**, 7260 (2000).
22. L. Cannavacciuolo, R. G. Winkler, and G. Gompper, EPL **83**, 34007 (2008).
23. R. Kekre, J. E. Butler, and A. J. C. Ladd, Phys. Rev. E **82**, 011802 (2010).
24. B. Z. Dlugogorski, M. Grmela, and P. J. Carreau, J. Non-Newtonian Fluid Mech. **48**, 303 (1993).
25. P. Peyla, EPL **80**, 34001 (2007); L. Jibuti, S. Rafai and P. Peyla, J. Fluid Mech. **693**, 345 (2012).
26. A. Celani, S. Musacchio, and D. Vincenzi, J. Stat. Phys. **118**, 531 (2005).
27. G. K. Fraenkel, J. Chem. Phys. **20**, 642 (1952).
28. H. R. Warner, Jr., Ind. Eng. Chem. Fundamen. **11**, 379 (1972).
29. S. I. Abdelkhalik and R. B. Bird, Appl. Sci. Res. **30**, 269 (1975).
30. E. J. Hinch and L. G. Leal, J. Fluid Mech. **71**, 481 (1975).
31. J. F. Brady, A. S. Khair, and M. Swaroop, J. Fluid Mech. **554**, 109 (2006).
32. P. Degond, A. Lozinski, and R. G. Owens, J. Non-Newtonian Fluid Mech. **165**, 509 (2010).
33. R. G. Winkler, Phys. Rev. Lett. **97**, 128301 (2006).
34. H. Tanaka and T. Araki, Phys. Rev. Lett. **85**, 1338 (2000).

35. T. Araki and H. Tanaka, Prog. Theor. Phys. Supp. 37 (2008).
36. K. Kamata, T. Araki, and H. Tanaka, Phys. Rev. Lett. **102**, 108303 (2009).
37. Y. Davit and P. Peyla, EPL **83**, 64001 (2008).
38. S. Rafai, L. Jibuti, and P. Peyla, Phys. Rev. Lett. **104**, 098102 (2010).
39. M. Doi and S. F. Edwards, *The Theory of Polymer Dynamics* (Clarendon Press, Oxford, 1986).
40. B. Kowalik and R. G. Winkler, J. Chem. Phys. **138**, 104903 (2013).
41. R. Peyret and T. Taylor, *Computational methods for fluid flow* (Springer, New York, 1990).
42. J. Happel and H. Brenner, *Low Reynolds Number Hydrodynamics* (Prentice-Hall, Englewood Cliffs, 1981).
43. T. C. B. Kwan and E. S. G. Shaqfeh, J. Non-Newtonian Fluid Mech. **82**, 139 (1999).